MODELING OF TURBULENT PREMIXED FLAMES IN THE FLAMELET REGIME

V. Kalyana Chakravarthy
School of Aerospace Engineering
Georgia Institute of Technology
Atlanta, Georgia 30332-0150
U.S.A

Thomas M. Smith
Parallel Computational Sciences Department
Sandia National Laboratory
Albuqurque, NM 87185
U.S.A

Suresh Menon
School of Aerospace Engineering
Georgia Institute of Technology
Atlanta, Georgia 30332-0150
U.S.A

ABSTRACT

Large eddy simulation (LES) models for flamelet combustion are analyzed by simulating premixed flames in turbulent stagnation zones. A LES approach based on subgrid implementation of the linear eddy model (LEM) is compared with a more conventional approach based on the estimation of the turbulent burning rate. The effects of subgrid turbulence are modeled within the subgrid domain in the LEM-LES approach and the advection (transport between LES cells) of scalars is modeled using a volume-of-fluid (VOF) Lagrangian front tracking scheme. The ability of the VOF scheme to track the flame as a thin front on the LES grid is demonstrated. The combined LEM-LES methodology is shown to be well suited for modeling premixed flamelet combustion. It is established here that local laminar propagation of the flamelets needs to be resolved in addition to the accurate estimation of the turbulent reaction rate. Some key differences between LES-LEM and the conventional approach(es) are also discussed.

INTRODUCTION

Premixed flames in the flamelet regime can be characterized by a laminar flame thickness (δ_f) which is much smaller than the smallest eddy size (Kolmogorov length scale η) in the turbulent flow field. Hence, the internal flame structure is unchanged by the fluid dynamics and the flame can be approximated as an infinitely thin surface convected by the local fluid velocity and propagating normal to itself at the laminar flame speed S_L. The task of modeling the flamelets is thus, reduced to the geometric tracking of the flame surface.

The flame surface is wrinkled by eddies of all sizes ranging from η to L (integral length scale). Each eddy causes the flame to wrinkle thus, increasing the flame surface area. Since the local propagation rate is S_L everywhere on the flame, the flame surface area is a direct measure of the turbulent burning rate. Although in principle, the effect of all energetic eddies on the flame surface wrinkling can be resolved by using direct numerical simulation (DNS), the resolution of a realistic high Reynolds number flame in a DNS is beyond the scope of present day computers (unless adjustments to the reaction rates are carried out to artificially thicken the flame structure). Here, a LES approach with a subgrid combustion model that avoids any ad hoc adjustments is developed and demonstrated for premixed flames in the flamelet regime.

In LES, only the eddies that are resolvable on the grid are simulated while the effects of unresolved turbulence on the large scale motion are approximated using a subgrid model. However, this approach is inapplicable for reacting flows since local consumption and flame wrinkling occur at the small scales in a highly localized fashion and their effects cannot be resolved and nor can be modeled by ad hoc means. Here, a model for the effect of unresolved turbulence on the flame-structure proposed by Menon et al. (1993) based on the linear eddy model of Kerstein (1989) is employed to study 3D premixed flames. Earlier, this model was used to model three dimensional flame kernels (Chakravarthy and Menon, 1997) and 2D stagnation point flames (Smith and Menon, 1998).

Turbulent premixed flame stabilized by a stagnating flow (a focus of this study) is a perfect candidate for studying turbulence-flame interactions. The turbulent flame brush is nearly planar and encounters turbulence that is homogeneous in the spanwise direction. Also, the turbulence intensity that the flame encounters can be controlled fairly accurately at the inlet (Cho et. al., 1986, 1988: Cheng and Shepherd, 1989). This is important because the effect of turbulence on the flame is quantized in terms of the turbulence intensity, which, in some configurations, may be difficult to measure (or control) at the flame location. This configuration is also suited

for computational studies since no bluff body, swirl or other stabilization mechanism is required and statistical stationarity of the flow field helps in data analysis. The simulations reported here are the first 3D LES of turbulent stagnation point flames under conditions identical to the experiments.

MODELING APPROACHES

The closure of the subgrid stresses in the LES equations (under zero-Mach number approximation) is carried out using an eddy viscosity model in terms of the filter width and the subgrid kinetic energy (Schumann, 1975). The subgrid kinetic energy is obtained by solving a modified version of the transport model given by Schumann (1975). The use of subgrid kinetic energy model not only helps to attribute a relaxation time (associated with non-equilibrium between production and dissipation of subgrid kinetic energy) for the subgrid scales, but also provides a measure for the local subgrid turbulence intensity (needed for flame-turbulence modeling, as discussed below).

The effect of the subgrid turbulence on the flame is modeled using the linear eddy model. The LEM-LES approach conducts one-dimensional LEM simulations in each LES cell, which can be considered a representation of the subgrid processes occurring within that cell at scales that cannot be resolved in a LES. Flame propagation within each LES cell is simulated using the G-equation model (Kerstein, 1988): $dG/dt = -S_L|\nabla G|$, where G is a progress variable taking values from 0 (fully reacted state) to 1 (reactant state). Thus, the flame is an infinitely thin surface between 0 and 1 and G can be related to the rate of advancement or the reaction progress variable C, i.e. $C = 1 - G$ and the temperature is assumed to be a linear function of C.

The effect of turbulent small-scale mixing in each LES cell is modeled stochastically using a turbulent stirring process described earlier (Menon et al., 1993: Kerstein, 1989). The key feature of this stirring process is that the length scale distribution and the associated frequency of the stirring events are chosen (Kerstein, 1989) so as to reflect the energy distribution among eddies of inertial range 3D turbulence. This capability allows LEM to capture 3D effects on scalar mixing (albeit stochastically) even though the subgrid domain is resolved in 1D. Recent studies show that this LES-LEM approach captures the topological structure of premixed flames (Menon and Kerstein, 1992) and the turbulent flame speed (Smith and Menon, 1996) quite accurately. More details of this subgrid implementation have been reported earlier (Menon et al., 1993: Chakravarthy and Menon, 1997; Smith and Menon, 1998) and are omitted here for brevity.

The large scale advection (due to the LES filtered velocity) of the scalar field is conducted using a Lagrangian volume transport method (similar to the front tracking method) and as detailed earlier (Smith and Menon, 1998). In this method, the LEM cells are transported from one LES cell to a neighboring LES to account for volume flux transport due to the fluid velocity at the interface of the two LES cells. The accuracy of this method in tracking scalar interfaces (thin fronts) has been established in earlier studies (Smith and Menon, 1998). The ability of the VOF scheme is demonstrated in figures 1 and 2. As shown, both passive advection and normal propagation (as in flames) of thin fronts are accurately captured.

LES using a subgrid flame-speed model is also conducted here to compare with the new LEM-LES approach. A filtered G equation model (Smith and Menon, 1998) is used for this purpose. The laminar propagation speed is replaced by the subgrid flame speed (that accounts for the increased flame area due to subgrid wrinkling). The subgrid flame-speed is the self-propagation speed of the G surfaces (isolevels) on the LES grid. The flame speed approach is typical of the reacting LES approaches (e.g., Kim et al., 1999) that estimate (using models) the subgrid turbulence effects on mixing (and/or reaction rates). The laminar propagation of the flamelets is however, not explicitly included in these methods. Thus, they differ significantly from the LEM-LES (which recognizes the need for modeling laminar propagation of the flamelets).

FLOW CONFIGURATION

The flow configuration consists of an axisymmetric turbulent jet of premixed reactants that is surrounded by an equal velocity laminar co-flow and impinging on a solid adiabatic wall placed 75 mm away from the jet inflow. The stagnating axial flow anchors a (near) planar turbulent flame brush above the wall. Isotropic turbulence is added to the uniform mean velocity (of 5 m/s) at the jet inflow (in order to mimic grid turbulence). The von Karman spectrum (at required intensity, u' and length scale, L) is used to construct the inflow turbulence. Since the jet is surrounded by an equal velocity co-flow, no shear layer is formed at the edges of the turbulent jet and hence, there is no significant turbulence production mechanism in the flow upstream of the flame. Thus, the turbulence that the flame encounters is directly correlated to the prescribed inflow turbulence.

Four parameter sets are chosen for analysis here. The parameters corresponding to simulations are shown in Table 1. Parameters used in simulations 1 and 2 are typical of experimental studies in the past (Cho et. al., 1986, 1988: Cheng and Shepherd, 1989). Hence, these two simulations would help in establishing the relative abilities of each method. The ratio of product to reactant temperatures (denoted by T_p and T_o, respectively) is set to 7 in all cases.

The solid boundary is assumed to be a no-slip, adiabatic wall and convective outflow conditions are used on the side boundaries. For analysis, only the core region of the flow (and the flame) is considered. The effect of the outflow boundary conditions on the flowfield in the core region is found to be negligible. Also, the thermal boundary layer at the wall is found to be very thin in the experiments and does not interfere with the flow in the vicinity of the flame

Table 1: SIMULATION PARAMETERS

Case	Method, Grid	S_L (cm/s)	Re_l	u'/S_L	N_B
1	FSM, 89x129x129	40	60	0.75	4.3
2	LEM-LES, 69x89x89	40	60	0.75	4.3
3	LEM-LES, 69x89x89	40	120	1.5	1.9
4	LEM-LES, 69x89x89	20	160	4.0	0.75
5	LEM-LES, 69x89x89	20	320	8.0	0.38

RESULTS and DISCUSSION

For cases 1 and 2, burning is customarily wrinkled flamelet type. The internal flame structure is undisturbed and the reaction zone is a single connected domain. The flame oscillates only slightly about it's mean position. For these cases, the contribution of subgrid turbulence to burning (subgrid wrinkling) is minimal. Case 2 is, therefore, a good test of the front tracking ability of the LEM-LES method. The progress variable distributions on one of the axial planes for cases 1 and 2 are shown in figure 3. The LEM-LES captures the flame as a thin wrinkled front whereas the flame is captured over a broader zone by the flame speed model (FSM) based simulation. The finite difference scheme in FSM leads to smoother wrinkles whereas the stochastic nature of (flame) area creation mechanism (subgrid stirring) in LEM-LES leads to a more wrinkled structure.

In cases 4 and 5, the burning is in a corrugated flamelet mode. The wrinkling is more 3D and some pockets of reactants separate from the main reaction zone and exist in isolation surrounded by the products. The transition from wrinkled to corrugated flamelet type is evident in figure 4.

The mean and the rms velocity profiles predicted by the LEM-LES and the conventional LES are compared to experimental data (Cho et. al., 1986, 1988: Cheng and Shepherd, 1989) in figures 5, 6 and 7. The mean velocity is predicted fairly well by both models but the prediction of turbulence is much better in case of LEM-LES. Across the flame, the density decreases significantly and this causes the flow to accelerate tremendously across the flame. This results in very high (flame normal) velocities on the product side (compared to the reactants side). The unsteady oscillations of the flame at any given point in the flame brush thus, causes very high intermittency which in turn leads to an increase in u'. This physics is captured quite accurately by the LEM-LES method. In the FSM method, the flame structure has a finite thickness which is determined by the numerics (grid, scheme, etc.) As a consequence, the flow acceleration (due to the density drop) is much more gradual than in the case of LES-LEM. This smoothening of the flow gradients reduces the flow intermittency and hence, the conventional approach does not produce the peak in u' at the flame brush as in the experiments and the LES-LEM simulation. This problem is also typical of LES that use finite-rate chemistry and transport equations for chemical species on the LES grid. At present, the resolution of δ_f in LES of any real flame on a 3D grid is impossible. Thus, the flamelet-type burning may never be captured using conventional methods. The LEM-LES method appears to achieve this goal due to the combination of the features of the subgrid LEM and the front tracking scheme.

Tangential strain rate on the flame surface is the most significant factor contributing to changes in surface area of premixed flames. The tangential strain rate (a_t) is primarily determined by the volumetric dilatation and the alignment of the flame normal relative to the local strain rate field. For passive flames in isotropic turbulence, the flame normal aligns most with the direction of minimum (principle) strain rate, a feature well captured by both the conventional and LEM-LES modeling approaches (Ashurst et al., 1987; Chakravarthy and Menon, 1997). However, in the presence of heat release the flame normal aligns more with the direction of maximum principle strain rate (maximum acceleration direction). This is not surprising given the fact that flow acceleration due to change in density would be primarily in the direction of the flame normal. The PDF of the flame normal (η) alignment with the direction of minimum (γ) and maximum (α) strain rates (over the whole flame surface) is shown in figure 8. It is seen that the alignment ($\alpha.\eta$) is higher in case of the LEM-LES and shows that the sharp velocity gradients across the flame are better captured in LEM-LES.

As the turbulence level increases (relative to S_L), the effects of turbulence dominate the effects of heat release. Due to the 3D fine-grained nature of wrinkles in high turbulence levels, the flow direction is more randomly oriented relative to the flame normal. Turbulent dynamics in such cases can lead to the local flow acceleration to be maximum in directions significantly away from the flame normal. Thus, the tendency of the flame normal to align with the local maximum principle strain rate direction is reduced and the alignment with minimum strain direction becomes more probable. This is illustrated by comparing flame-strain rate alignment PDFs for cases 4 and 5 shown in figure 9 with figure 8.

The PDFs of the tangential strain rate (normalized by the mean inflow velocity and axial length of the computational domain) on the flame surface for the LEM-LES cases are shown in figure 10. It is seen that the local strain rates on the flame surface typically increases with increasing u'. The phenomenon of local extinction (not modeled here) which occurs due to a_t becomes a significant factor at high turbulent intensities. In order to determine the size of the eddies most effective in leading to thermal extinction, the

tangential strain rate PDFs are re-plotted in figure 11 by normalizing them with the corresponding Kolmogorov time scales (τ_{kol}). In general, $\tau_{kol}a_t$ is seen to reduce with increase in u'. This trend is explained as follows. At fixed Kolmogorov scale, the range of turbulent eddy sizes (η-L) increases with increasing u'. So the tangential strain rate PDF should reflect the presence of large eddies at high u'. Since the PDF shifts to the left, it can be argued that the energy distribution among eddy sizes is such that the strain rate produced by large eddies is less than that caused by smaller eddies. It is generally known that extinction (in most cases) is caused by very fine (i.e. small) scale eddies. The LEM-LES predictions are in agreement with this observation.

The turbulent flux, $\rho<u_i''C''>$, where $< >$ represents a Favre filter), plays a dominant role in determining the reactant and product mixing and thus, the flame structure and consumption rate in premixed flames. This term is usually modeled using a gradient diffusion assumption. However, the presence of counter-gradient diffusion in premixed flames is now well established from experiments (Cho et al., 1988; Li et al., 1994) and direct simulations (Veynante et al., 1997). The nature of turbulent diffusion was found to be primarily dependent on the Bray number, N_B:

$$N_B = \left\{\frac{T_p}{T_o} - 1\right\}\frac{S_L}{2\alpha u'}$$

where α is an efficiency factor that asymptotes to 1 as $L/\delta_f \to \infty$ (which is the case here) . The Bray numbers for the various cases are shown in Table 1. It is seen that counter-gradient diffusion primarily occurs at lower u', when $N_B>1$. At higher u', turbulent diffusion is in the direction of the scalar gradient ($N_B<1$). The turbulent flux variations along the axial line for the LEM-LES cases are shown in figure 12. As shown, counter-gradient occurs in cases 2 and 3 and gradient diffusion occurs in cases 4 and 5. The LEM-LES results are consistent with predictions based on Bray number noted in the past.

CONCLUSIONS

The results reported here demonstrate that resolution of the flame plays a key role in determining flame-turbulence interactions in LES. Although the subgrid flame speed estimate (using Yakhot's model or any other model) may be accurate, the flamelet propagation needs to be modeled for improved accuracy. The subgrid propagation simulated in LEM, along with the VOF front tracking scheme used in LEM-LES, is found to be fairly accurate in capturing key features of flamelet combustion. Although the G equation is used in the current work, the observations made here have similar implications for LES that use finite-rate chemistry. The resolution of the flame structure along with an accurate estimate of subgrid reaction rates is essential for modeling premixed flames in any type of LES.

It is also established that turbulent diffusion is modeled accurately in LES as opposed to Reynolds-averaged approach. The inherently unsteady nature of turbulent combustion makes Reynolds-averaged approaches highly unsuitable for combustion modeling. Another purpose of this paper has been to highlight the essential differences between conventional LES and the present LEM-LES approach. Further analysis of the flame geometry and flame-turbulence interactions are being conducted and will be reported in the future.

ACKNOWLEDGEMENTS

This work was supported in part by NASA Lewis Research Center under the Microgravity Combustion Program and by the Army Research Office under the Multidisciplinary University Research Initiative. Computational support was provided by the DoD High Performance Computing Center at SMDC, Huntsville, AL, under a Grand Challenge Project.

REFERENCES

Ashurst, W., Kerstein, A. R., Kerr, A., and Gibson, C., 1987 , "Alignment of vorticity and scalar gradient with strain rate in simulated Navier-Stokes turbulence," *Physics of Fluids*, Vol. 30, No. 8, pp. 2343 - 2353.

Chakravarthy, V. K., and Menon, S., 1997, "Characteristics of a subgrid model for turbulent premixed combustion," AIAA-97-3331.

Cheng, R., and Shepherd, I., 1989, "A comparison of the velocity and scalar spectra in premixed turbulent flames," *Combustion and Flame*, Vol. 78.

Cho, P., Law, C. K., Hertzberg, J., and Cheng, R., 1986, "Structure and propagation of turbulent premixed flame stabilized in a stagnation flow," *Twenty-first Symposium (International) on Combustion*, pp. 1493 - 1499.

Cho, P., Law, C., Cheng, R., and Shepherd, I., 1988, "Velocity and scalar fields of a turbulent premixed flame stabilized in a stagnation flow," *Twenty-second Symposium (International) on Combustion*, pp. 739 - 745.

Kerstein, A. R., Ashurst, W., and Williams, F., 1988, "Field equation for interface propagation in an unsteady homogeneous flow field," *Physical Review A*, Vol. 37, pp. 2728 - 2731.

Kerstein, A. R., 1989, "Linear eddy model of turbulent transport II," *Combustion and Flame*, Vol. 75, pp. 397 - 413.

Kim, W.-W., Menon, S. and Mongia, H. C., 1999, "Large eddy simulation of a gas turbine combustor flow," *Combustion Science and Technology* (to appear).

Li, S., Libby, P., and Williams, F., 1994, "Experimental investigation of a premixed flame in an impinging turbulent stream," *Twenty-fifth Symposium (International) on Combustion*, pp. 1207 - 1214.

Menon, S., McMurtry, P., and Kerstein, A. R., 1993, "A linear eddy mixing model for LES of turbulent combustion," in *LES of Complex Engineering and Geophysical flows*, edited by B. Galperin and S. Orszag, Cambridge Univ. Press, pp. 287-317.

Menon, S., and Kerstein, A. R., 1992, "Stochastic simulations of the structure and propagation rate of turbulent premixed flames," *Twenty-Fourth Symposium (International) on Combustion*, pp. 443-450.

Schumann, U., 1975, "Subgrid scale model for finite difference simulations of turbulent flows in plane channels and annuli," *Journal of Computational Physics*, Vol. 18, pp. 376- 404.

Smith, T.M., and Menon, S., 1996, "One-dimensional simulations of freely propagating turbulent premixed flame," *Combustion Science and Technology*, Vol. 128, pp. 99-130.

Smith, T.M., and Menon, S., 1998, "Subgrid combustion modeling for premixed turbulent reacting flows," AIAA-98-0242.

Veynante, D., Trouve, A., Bray, K., and Mantel, K., 1997, "Gradient and counter gradient scalar transport in turbulent premixed flames," *Journal of Fluid Mechanics*, Vol. 332, pp. 263 - 293.

Yakhot, V., 1988, "Propagation velocity of premixed turbulent flames," *Combustion Science and Technology*, Vol. 60, pp. 191 - 214.

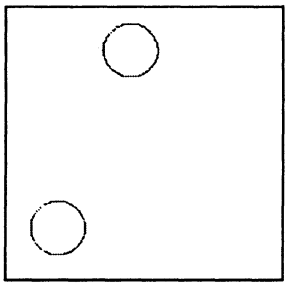

Figure 1: Convection in an arbitrary direction of a sharp circular front by uniform flow

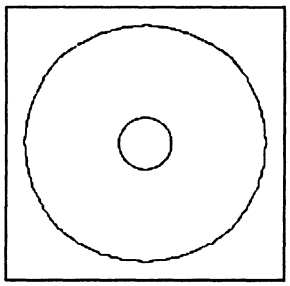

Figure 2: Outward propagating circular flame front at a fixed flame speed

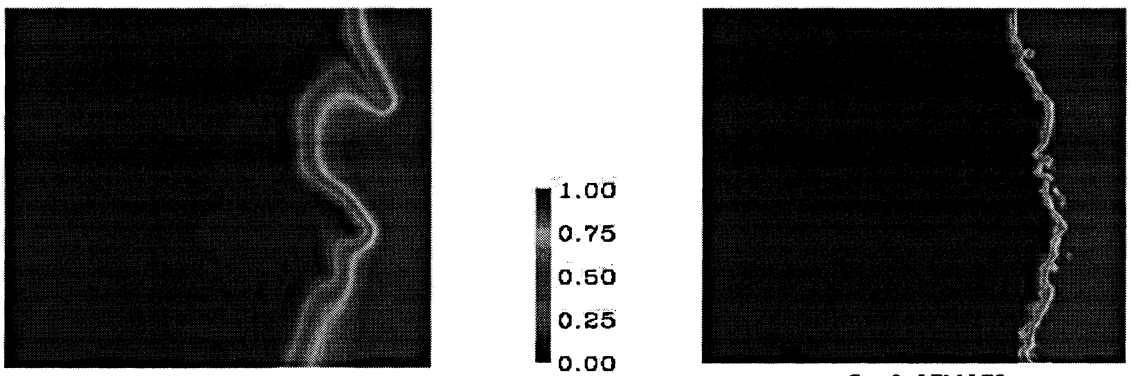

Case 1 : LES using a flame-speed model

Case 2 : LEM-LES

Figure 3: Instantaneous flame structure (progress variable fields)

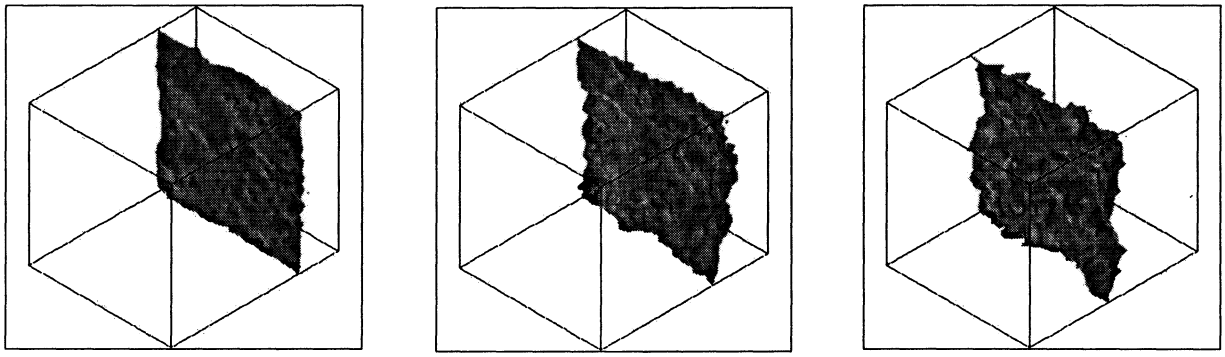

Case 3 : $u'/S_L = 1.5$

Case 4 : $u'/S_L = 4$

Case 5 : $u'/S_L = 8$

Figure 4: Transition of flame structure from wrinkled flamelet type to corrugated type with increasing u'/S_L

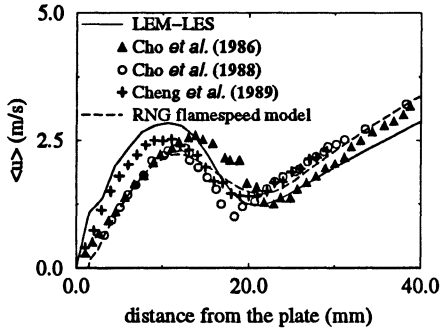

Figure 5: Mean axial velocity predictions on the center-line

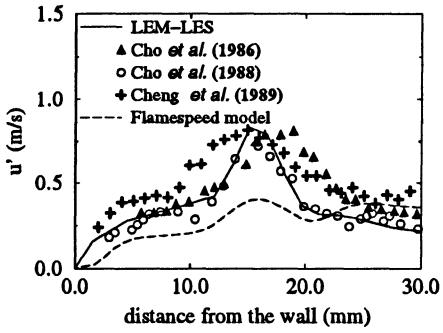

Figure 6: *rms* axial velocity predictions on the center-line

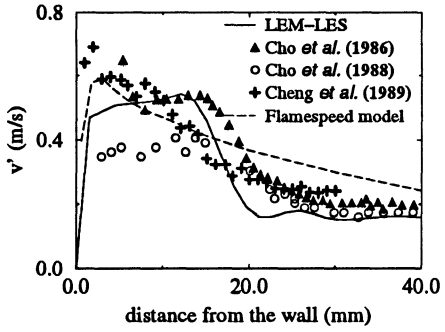

Figure 7: *rms* radial velocity predictions on the center-line

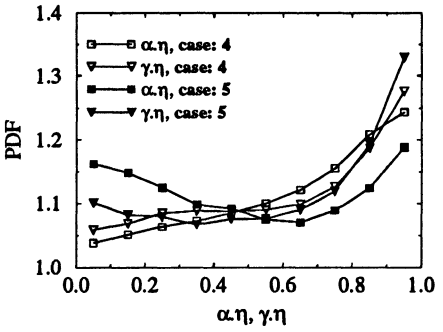

Figure 8: Flame alignment with directions of maximum and minimum principle strain rates in the wrinkled flamelet regime.

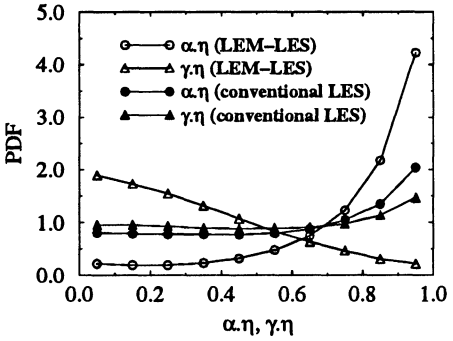

Figure 9: Flame alignment with directions of maximum and minimum principle strain rates in corrugated flamelet regime

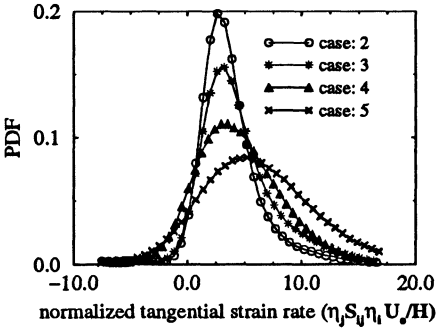

Figure 10: PDF of tangential strain rates on the flame surface

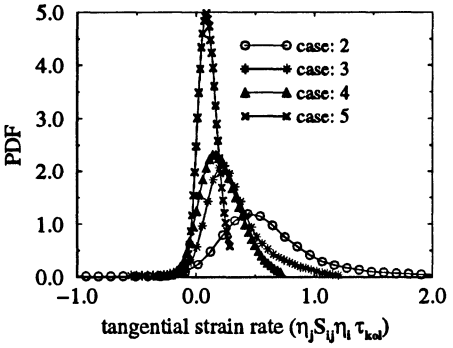

Figure 11: Kol-time scale normalized tangential strain rate

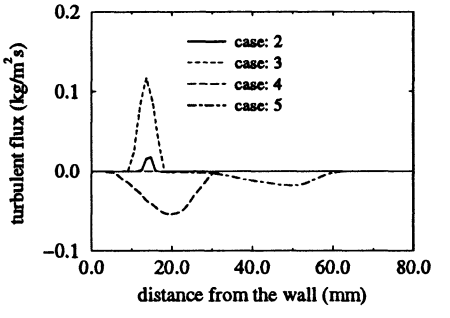

Figure 12: Turbulent mass flux along the center-line.